Applied Microbiology and Biotechnology (2025) 109:69
https://doi.org/10.1007/s00253-025-13445-x

APPLIED MICROBIAL AND CELL PHYSIOLOGY

Bifidobacterium lactis ameliorates AOM/DSS-induced inflammation, dysbiosis, and colonic precancerous lesions

Yi-Lin Chan[1] · Jun-Cheng Liao[2] · Tsung-Lin Li[3] · Chang-Jer Wu[4,5] · Yi-Han Chiu[2]

Received: 13 March 2024 / Revised: 25 February 2025 / Accepted: 25 February 2025

Abstract

Bowel cancer is the third most common malignancy of tumors and one of the major causes of cancer-related death. Bowel precancerous conditions can develop without any symptoms, which either makes it difficult for early diagnosis or poses a poor prognosis/gloomy relapse. This study aimed to investigate the effects of *Bifidobacterium animalis* subsp. *lactis* TCI604 (*B. lactis*) on inflammatory responses, gut microbiome, and protectiveness against azoxymethane (AOM)/dextran sodium sulfate (DSS)-induced colonic precancerous lesions. The AOM/DSS-induced colonic precancerous lesion murine model was studied with 24 female C57BL/6 J mice assigned to the control group, AOM/DSS-induced colonic precancerous lesion group (AOM/DSS), AOM/DSS treated with *B. lactis* probiotic group (*B. lactis* P), and AOM/DSS treated with *B. lactis* cell-free supernatant group (*B. lactis* S). The results showed that both *B. lactis* P and *B. lactis* S could attenuate AOM/DSS-induced body weight loss and intestine damage, reduce aberrant crypt foci (ACF) and the formation of colonic polyps, and significantly inhibit pro-inflammatory cytokines and the NF-κB signaling pathway, in which the *B. lactis* S group outperformed others. Further analysis using 16S rDNA sequencing suggested that both *B. lactis* P and *B. lactis* S optimize gut microbiota. Several bacteria, including *Muribaculaceae*, *Prevotellaceae_UCG-001*, *Anaerostipes*, *Ruminococcaceae*, *Mucispirillum*, *Clostridia_UCG-014*, and *Clostridia_vadinBB60* that were known in close relation to colonic precancerous lesions, were sequenced at taxonomic level. Our results indicated that both *B. lactis* P and *B. lactis* S improved AOM/DSS-induced colonic precancerous lesions by regulating inflammation as well as optimizing gut microbiota, thereby establishing reciprocally cooperative net benefits between probiotics/postbiotics and mice with colonic precancerous lesions.

Key points

- *Prophylactic administration of probiotic and postbiotic of B. lactis is capable of alleviating the AOM/DSS-induced body weight loss and colon shortening, as well as diminishing the development of colonic precancerous lesions, such as the formation of ACF and colonic polyps, in an AOM/DSS mouse model*
- *Either probiotic or postbiotic of B. lactis has a positive role in mediating immune imbalance and colonic inflammation via suppression of inflammatory immune cells, pro-inflammatory cytokines, and the NF-κB signaling pathway*
- *AOM/DSS-induced dysbiosis can be reversed with the probiotic and postbiotic of B. lactis supplementation*

Keywords *Bifidobacterium animalis* subsp. *Lactis* · Probiotics · Postbiotics · Colonic precancerous lesions · Gut microbiota

✉ Chang-Jer Wu
cjwu@mail.ntou.edu.tw

✉ Yi-Han Chiu
chiuyiham@scu.edu.tw

[1] Department of Chemistry, Chinese Culture University, Taipei, Taiwan, ROC

[2] Department of Microbiology, Soochow University, 70, Linhsi Road, Taipei, Taiwan, ROC

[3] Genomics Research Center, Academia Sinica, Taipei, Taiwan, ROC

[4] Department of Food Science and Center of Excellence for the Oceans, National Taiwan Ocean University, 2, Pei Ning Road, Keelung, Taiwan, ROC

[5] Graduate Institute of Medicine, Kaohsiung Medical University, Kaohsiung, Taiwan, ROC

Published online: 21 March 2025

Introduction

Bowel cancer is the third most common malignancy of tumors to treat and one of the major causes of cancer-related death (Xi and Xu 2021). Risk factors related to diet and behavior (Butler et al. 2003), inflammatory bowel disease (Porter et al. 2021), colonic polyps (Stryker et al. 1987), hereditary polyposis (Kanth et al. 2017), and familial colorectal cancer (Ponz de Leon et al. 2004) are major factors in association with the development of bowel cancer. Managing these hazardous factors helps lower the risk of developing bowel cancer, while bowel precancerous conditions often develop silently with no symptoms, thus making bowel cancer difficult to diagnose early and leading to a gloomy relapse/poor prognosis. Finding early biomarkers in neoplastic or dysplastic colon epithelium ought to be of great interest.

The process of colon carcinogenesis involves a sequence of changes from a healthy mucous membrane to excessive proliferation, aberrant crypt foci (ACF), and the formation of colonic polyps on route to malignant transformation. Numerous studies have shown that the higher the number of adenomas, the more dysplastic ACF there are in patients (Takayama et al. 1998). ACF found around adenomas is analogous to adenomas found at the periphery of colon carcinoma (Brenner et al. 2007). Given the fact that ACF is an early preneoplastic lesion in the "ACF-adenoma-carcinoma" sequence, the size and number of crypts per focus are directly correlated with the risk of bowel cancer (Wargovich et al. 2010).

Colonic polyps are considered the precursors of colon cancer in view of similar histology and gene profile with those of dysplastic ACF. A previous cohort study revealed that 131 dysplastic ACF patients who had a high number of ACF were well correlated with adenoma patients with a high number of hyperplastic polyps (Kowalczyk et al. 2020). A colonic polyp is defined as a protuberance in the lumen above the adjacent colonic mucosa, which is asymptomatic at first but may result in an ulcer with bleeding (Potet and Soullard 1971). Colonic polyps are histologically classified into neoplastic (adenomas polyps) and non-neoplastic (inflammatory polyps). The presence of colonic neoplasms in the inner wall of the colon is the most common and critical type of adenomatous polyps that often develop into bowel cancer (Shussman and Wexner 2014). The mechanism by which adenomatous polyps raise the risk of bowel cancer is still unclear. Most patients with adenomatous polyps appear to result from genetic factors entangling with environmental factors, leading to colonic malignant transformation and then bowel cancer (Wasif et al. 2011). There are three main histologic variants of adenomatous polyps: (1) tubular adenomas, the most common (75–85%) diminutive polyp (diameter ≤ 5 mm), have $< 5\%$ malignant potential, (2) tubulovillous adenomas account for 10–15% of polyps with 20–25% malignant potential, and (3) villous adenomas constitute 5–10% of overall polyps, which are often large (diameter > 20 mm) with 35–40% malignant potential (Amersi et al. 2005). Given the size, histology, and propensity for dysplasia, the tubular adenomas that develop into adenocarcinomas are more than occasional. Polyps larger than 20 mm have $> 40\%$ of chance morphing into malignant lesions, and 35% of polyps with severe dysplasia are malignant after complete excision. On top of that, the 5- and 10-year carcinogenesis rates of adenomatous polyposis are as high as 4 and 14%, respectively (Wasif et al. 2011), exceeding expectations for the normal population. Therefore, there is an unmet medical need for early and effective detection of premalignant polyps and colon cancer.

Regular colonoscopy surveillance and surgical removal are the most effective ways to manage adenomatous polyps as well as reduce the risk of bowel cancer. Recently, the use of probiotics has been hailed as a breakthrough in decreasing adenomatous polyps and preventing bowel cancer as manifested in both animal and human applications. For example, supplementation for 10 weeks with an admixture of *Lactobacillus acidophilus* (NCFM®), *Lactobacillus paracasei* (Lpc 37TM), *Bifidobacterium lactis* (Bi-04TM), *Bifidobacterium lactis* (Bi-07TM), and *Bifidobacterium bifidum* (Bb-02TM) in rat model bearing chemically induced colon cancer decreased the formation of aberrant crypts, ameliorated tumor malignancy, and enhanced the antitumor effect of 5-fluorouracil chemotherapy; otherwise, it led to the occurrence of neoplastic lesions (Genaro et al. 2019). A metagenomic study reported that the consumption of *Lactobacillus rhamnosus* GG (LGG) helped maintain the overall functional potential and taxonomic profile of resident microbes, increasing short-chain fatty acid (SCFA) production and decreasing 25% total polyp counts in the $Apc^{Min/+}$ mice model (Ni et al. 2017). Furthermore, a colonoscopy-based case–control study revealed that the odds of hyperplastic polyp were reduced with daily yogurt intake, and the odds of adenomatous polyp were decreased with weekly yogurt intake (Rifkin et al. 2020).

Probiotics, such as *Lactobacillus* and *Bifidobacterium*, have been shown to benefit digestive disorders (Skrzydło-Radomańska et al. 2020; Szajewska and Hojsak 2020), while their use in bowel cancer is still inconclusive. Several mechanisms, including pro-apoptosis (Sugimura et al. 2021), carcinogen inactivation (Liu et al. 2021), alteration of microbial community and metabolism (Gomes et al. 2022), and modulation of host immune responses, have been proposed in an endeavor to understand the preventive effect of probiotics against bowel cancer (Owens et al. 2021). It is likely that a given probiotics works with a specific mechanism (Uccello

et al. 2012; Lin et al. 2009). *Bifidobacterium animalis* subsp. *lactis* (*B. lactis*) is the most extensively studied species that secretes folic acid, peroxides, and bacteriocins (D'Aimmo et al. 2012; Oberg et al. 2013; Martinez et al. 2015), helps transform minerals into bioavailable forms (Mogna et al. 2012), and fortifies barrier functions in gut defenses (Cheng et al. 2021), thus promoting digestive wellness, such as ameliorating diarrhea and constipation. Nevertheless, the preventive colonic neoplasm mechanism in association with *B. lactis* remains largely unclear. The present study was therefore set to investigate the immune-modulatory benefits, the colonic precancerous preventive mechanism of *B. lactis*, and its postbiotic effects on the AOM/DSS-induced colon carcinogenesis murine models.

Materials and methods

Bacterial strains, test preparations, and growth conditions

The *Bifidobacterium* strain (*Bifidobacterium animalis* subsp. *lactis* TCI604) and its cell-free supernatant were provided by TCI CO., Ltd., Taipei, Taiwan. *B. lactis* TCI604 were grown at 37 °C in MRS broth (Difco, Sparks, MD, USA) and were cultured to reach the bacterial density of 10^9 colony-forming units/ml, harvested by centrifugation (10,000 × *g* for 30 min), washed with PBS, and then orally administered to mice as a suspension in 1X PBS. The suspended *B. lactis* bacterial strain was used for the in vivo study.

Ethical approval and animals.

Female C57BL/6 J mice (5 weeks) were obtained from the National Laboratory Animal Center (Taipei, Taiwan, ROC) and underwent a 1-week adjustment to a new environment and diet before treatments were performed. Food and water were given ad libitum. Mice were maintained humanely and ethically, in accordance with regulations of the Institutional Animal Care and Use Committee (IACUC) at National Taiwan Ocean University (NTOU), and the study conformed to the guidelines of the protocol IACUC-110035 approved by the IACUC ethics committee of NTOU. All experiments were performed on C57BL/6 J mice ordered from the National Laboratory Animal Center (NLAC, Taipei, Taiwan).

AOM/DSS murine model of colonic precancerous lesions

The study process is outlined in Fig. 1. The mice were randomly divided into four groups: control group, AOM/DSS-induced colonic precancerous lesion group (AOM/DSS), AOM/DSS-induced colonic precancerous lesions treated with *Bifidobacterium animalis* subsp. *lactis* TCI604 probiotic group (*B. lactis* P), and AOM/DSS-induced colonic precancerous lesions treated with *B. lactis* TCI604 cell-free supernatant group (*B. lactis* S). Each group consisted of six mice. Modeling of AOM/DSS-induced colonic precancerous lesions was carried out according to protocol (Arnesen et al. 2021). The mice in the AOM/DSS, *B. lactis* P, and *B. lactis* S groups receive intraperitoneal (i.p.) injection with a single dose of AOM (10 mg/kg body weight) on the first day, and thereafter, three cycles of the inflammatory agent 2% (w/v) dextran sulfate sodium salt (DSS; MP biomedicals, Solon-Ohio, Burlingame CA) in drinking water were administered. For each cycle of DSS, the mice in the AOM/DSS, *B. lactis* P, and *B. lactis* S groups received water containing 2% DSS (w/v) for 5 days in a row, followed by 2 weeks of sterile water. DSS-induced mice colonic precancerous lesions were stimulated by 2% DSS in drinking water ad libitum as described elsewhere. To study the effect of *Bifidobacterium* factor treatment on the experimental colonic precancerous lesions, mice received live bacteria (*B. lactis* P) (1×10^8 CFUs/ day) or *B. lactis* TCI604 cell-free supernatants (80 µg/day) diluted in 200 µl PBS once a day by intragastric gavage from the first day post-AOM i.p. injection to the day before killing. The control group received the equivalent volume (200 µl) of phosphate-buffered saline (PBS) by intragastric gavage. On day 79, mice under anesthesia were exsanguinated, where the plasma was collected, and the small and large intestine organs were removed, weighed, their lengths measured, and then frozen immediately in liquid nitrogen for later analysis.

Blood sample analysis

Blood samples (0.5 ml) for measurements of red blood cells (RBCs), hemoglobin, mean corpuscular hemoglobin concentration (MCHC), white blood cells (WBCs), and absolute neutrophil, eosinophil, monocyte, and lymphocyte counts were determined by a blood cell analyzer (Symex K-1000, Sysmex American, Mundelein, IL, USA).

Flow cytometry

During flow cytometry, at least 5×10^5 splenocytes were analyzed by BD Accuri C6 flow cytometer with CFlow plus software (BD Biosciences, San Jose, CA, USA). Lymphocytes were gated based on the expression of CD3 and CD4 or CD8. B cells were gated based on the expression of CD19. NK cells were gated based on the expression of CD314.

Western blot analysis

Colon tissues were lysed with 0.5 ml of CelLytic M lysis reagent (Sigma-Aldrich) containing 1% phosphatase inhibitor cocktail (Sigma-Aldrich) and protease inhibitor cocktail

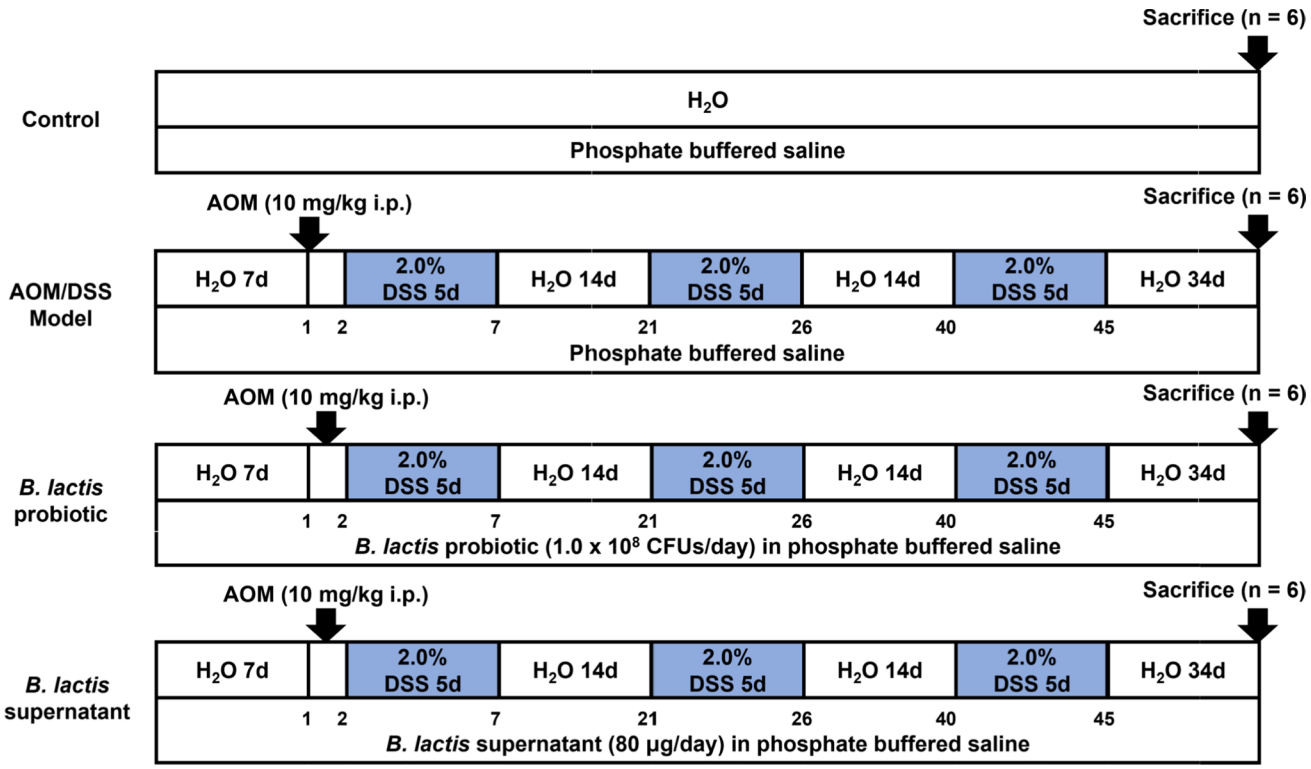

Fig. 1 Schematic representation of multistep carcinogenesis progression in the AOM/DSS murine model. C57BL/6 J mice were given a single i.p. injection of AOM (10 mg/kg) on the first day and provided drinking water ad libitum containing 2% (w/v) DSS for 5 days, followed by 2 weeks of sterile water. Mice were subjected to three cycles of 2% DSS (5 days per cycle) treatment and regular water (14 days per cycle). The total experimental period was 79 days. *B. lactis* P (1×10^8 CFUs/day) or *B. lactis* S (80 µg/day) were orally inoculated 7 days before AOM treatment and continued supplement for 79 days

(Sigma-Aldrich). Then, each sample was centrifuged at 13,000 × *g* for 30 min at 4 °C. The rapid Coomassie Kit (Bio-Rad) determined the total protein concentration. Apply cell lysates to a 10% SDS-PAGE, and then transfer onto a PVDF membrane, followed by incubation with specific primary antibodies against IκB-α, NF-κB, IKK-β, and GAPDH (all purchased from iReal, Taipei, Taiwan), accordingly. Subsequently, the PVDF membranes were incubated with secondary antibodies for 1 h at room temperature. Internal controls were GAPDH. Immunoreactive proteins were visualized by Immobilon™ Western chemiluminescent HRP Substrate kit (Millipore, MA, USA). Images were captured, and the intensities of the protein bands analyzed using the Lab works® software (V4.5, UVP Inc., Upland, CA, USA) are expressed as arbitrary optical density units.

ELISA assay

A multiplex ELISA kit (DuoSet, R & D systems, Minneapolis, MN, USA) was used to evaluate the levels of the cytokines, IL-1β, IL-6, IL-10, TNF-α, and IFN-γ, in the colon homogenates of the animals. The assay was performed according to the manufacturer's instructions in colon homogenate.

Histopathological analysis

Colon tissues were collected from mice, washed carefully with cold normal saline 3 times, then fixed in formalin solution 10%, processed, and embedded in a paraffin film. Sections of 5-µm-thick slices of tissues were prepared. The sections were stained with H&E. Microscopic observations were carried out at × 200 magnifications.

Quantification of macroscopic intestinal polyps

Following sacrifice, the large intestine was removed and flushed with PBS from both sides using blunt-end gavage needles to remove fecal material. Each colon tissue was then cut open longitudinally. Typical polyps were photographed when the intestines were open. The unstained large intestine was examined by two investigators to determine the polyp number and size.

DNA extraction and sequencing

The extraction method for bacterial DNA was performed using a stool DNA Isolation Kit (Qiagen, Hilden, Germany), following the manufacturer's instructions. Extracts were then treated with DNase-free RNase to eliminate RNA contaminants. The DNA yield and quality were measured by Pico-Green and Nanodrop (Thermo Fisher Scientific, Inc., Pittsburgh, PA, USA). Input genomic DNA (10 ng) was amplified by polymerase chain reaction (PCR). The barcoded fusion primers 341F (5′-CCTACGGGNGGCWGCAG −3′) and 805R (5′-GACTACHVGGGTATCTAATCC-3′) were used to amplify the V3 and V4 regions (341F-805R). The final purified product was then quantified using quantitative PCR (qPCR) according to the qPCR Quantification Protocol Guide (KAPA Library Quantification kits for Illumina 16S Metagenomic Sequencing Library), and the quality was checked using the Qubit 2.0 Fluorometer (Thermo Scientific, Waltham, MA, USA) and an Agilent Bioanalyzer 2100 system. The final library was sequenced using a 2×300 bp paired-end protocol for the MiSeq platform (Illumina, San Diego, CA, USA). Raw data were uploaded as FASTQ files after demultiplexing of paired-end reads. Sequencing results in the form of FASTQ files were uploaded to the MetaGenome Rapid Annotation Subsystems Technology (MG-RAST) server for analysis. Illumina metagenomic datasets are available on the NCBI under the Bioproject accession PRJNA1095174.

Bioinformatics analysis

Paired-end reads (2×300 bp) were trimmed by Trimmomatic (v0.39) (Bolger et al. 2014) and demultiplexed by in-house script. Sequences from both ends of 341F-805R primers were trimmed by Cutadapt (v3.3) with the following criteria: read length ≥ 150 bp and error rate 0.1 as default. DADA2 (v1.12) (Callahan et al. 2016) was subsequently used to perform preprocessing, which includes filtering out noisy sequences (denoise), merging paired-end reads, and removing chimera to extract amplicon sequence variants. The operational taxonomic unit (OTU) number was determined by clustering the sequences from each sample using a 97% sequence identity cut-off using the QIIME2 naive-Bayes classifier (v2019.10). The alpha diversity was analyzed by a species richness estimator (Chao1 and observed features) and a species evenness estimator (Shannon and Simpson) by using the vegan R package, and principal component analysis (PCA) was performed after applying the covariance matrix through the identification of differences between organism compositions for beta diversity. Taxonomic abundance was calculated using the QIIME2 naive-Bayes classifier (v2019.10) from the reads of each processed sample.

Statistical analysis

All bioinformatics analyses were performed in a vegan R package; graphics were conducted in R using the package ggplot2. QIIME feature tables and taxonomic assignments for the ASV and OUT datasets were imported into phyloseq via qiime2R for downstream analyses.

All experiments were performed at least in triplicate. Statistical differences were analyzed using GraphPad Prism, version 8.0 for Windows (GraphPad Software, La Jolla, California, USA) by performing a one-way ANOVA test. A p-value of less than 0.05 was considered statistically significant.

Results

B. lactis attenuate DSS-induced body weight loss in mice

The changes in body weights for test animals during the experimental course are summarized in Fig. 2. In general, the body weight of mice decreased substantially at each periodic exposure to DSS, and the mice tentatively regained their body weight once the DSS treatment was suspended. From the second exposure to DSS onward, the body weight loss of the mice in the AOM/DSS, *B. lactis* P, and *B. lactis* S groups was diminished significantly, suggesting an adaptive and cooperative recovery from inflammation under the DSS stimulation. After the third exposure to DSS, the body weight of AOM/DSS mice decreased significantly in stark contrast to those of the mice groups receiving either *B. lactis* P or *B. lactis* S, which showed body weight loss to a lesser extent ($p<0.05$), suggesting *B. lactis* P or *B. lactis* S exerts its effects on restoring the body weight from the DSS-induced weight loss (Fig. 2).

Prevention of AOM/DSS-induced small and large intestine damage, aberrant crypt foci, and formation of colonic polyps by *B. lactis*

AOM/DSS-induced intestinal damage was evaluated by measuring the length and weight of small and large intestines, ACF, and colonic polyps. The length of the small intestine in AOM/DSS mice is shorter than those in the control, *B. lactis* P, and *B. lactis* S groups ($p<0.05$, Fig. 3A, B). The colon lengths were 7.17 ± 0.60 cm, 5.63 ± 0.56 cm, 6.80 ± 1.02 cm, and 5.53 ± 0.69 cm for the control group, the AOM/DSS group, the *B. lactis* P group, and the *B. lactis* S group, respectively. On average, the colon length of the control mice was 27.35% longer than those of mice treated with AOM/DSS. Mice subjected to the AOM/DSS treatment exhibited a reduction in colon

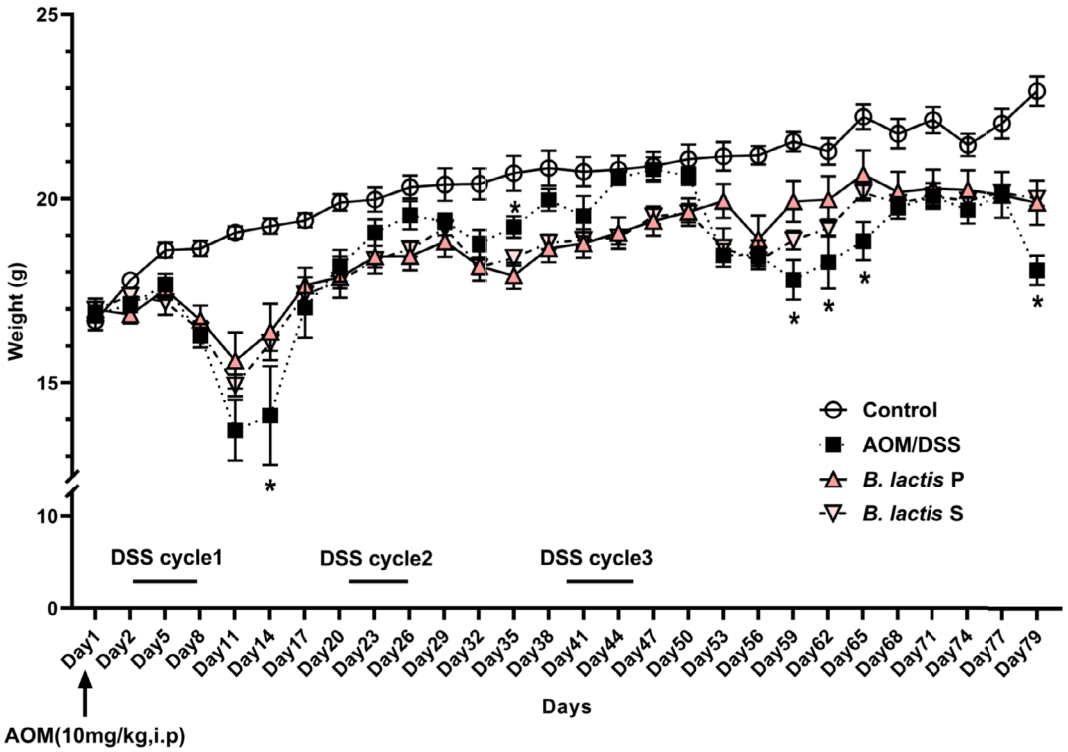

Fig. 2 Weight changes of mice among four groups. C57BL/6 J mice were given a single i.p. injection of AOM (10 mg/kg) on the first day and provided drinking water ad libitum containing 2% (w/v) DSS for 5 days, followed by 2 weeks of sterile water. Mice were subjected to three cycles of 2% DSS (5 days per cycle) treatment and regular water (14 days per cycle). The total experimental period was 79 days. *B. lactis* P (1×10^8 CFUs/day) or *B. lactis* S (80 μg/day) were orally inoculated 7 days before AOM treatment and continued supplement for 79 days. Data are expressed as the means ± SD. *$p < 0.05$ significantly different from the control group

length, whereas those receiving the *B. lactis* P treatment improved their colon length by 20.72% when compared with that of the AOM/DSS group ($p < 0.05$, Fig. 3D, E) but comparable to that of the *B. lactis* S administration ($p > 0.05$, Fig. 3D, E). Our results suggested that the treatment with *B. lactis* P could reverse the AOM/DSS-induced colon shortening.

The colonic precancerous lesions in the mice under the treatment of AOM/DSS were assessed for their colon mucosa proliferation and polyp occurrence at macroscopic and microscopic levels (Fig. 4). Colonic polyps (with a characteristic opaque spot) emerged from colons in all AOM/DSS mice (100%, Fig. 4A); macroscopic observation revealed that mucosal protuberance was increased in the descending colon region (Fig. 4B). Interestingly, with addition of *B. lactis* P or *B. lactis* S, both number and size of polyps were reduced in colon (Fig. 4A, B).

We then examined what effects could result with respect to the weight changes of the small/large intestines and the formation of colonic polyps when AOM and DSS were applied. The weight of the small intestine in all groups is similar ($p > 0.05$, Fig. 3C), suggesting that AOM/DSS did not cause a significant weight change in the small intestine. The colon weights for the control, AOM/DSS, *B. lactis* P, and *B. lactis* S groups were measured as 0.18 ± 0.04, 0.22 ± 0.05, 0.18 ± 0.046, and 0.18 ± 0.02 g, respectively, where the one in the AOM/DSS group is significantly higher than others ($p < 0.05$, Fig. 3F). The increased colon mass is proportional to the increased polyp mass, where the mean number of colonic polyps treated by AOM/DSS, AOM/DSS + *B. lactis* P, and AOM/DSS + *B. lactis* S is 12.2 (range 8–17), 4.5 (range 2–6), or 4.2 (range 2–7), respectively (Fig. 4A–C, $p < 0.05$). It is worth noting that the colon sections of AOM/DSS mice showed a noticeable increased number and size of polyps in agreement with the macroscopic observation. The number of colonic polyps reflects what type of treatment; likewise, the colon weight is positively proportional to the number of polyps in the colon (Fig. 4D, $r = 0.746$, $p < 0.001$). As shown in Fig. 4E, the H&E staining is consistent with the descriptions mentioned above; namely, the polyp load is decreased in the mice treated with *B. lactis* P and *B. lactis* S.

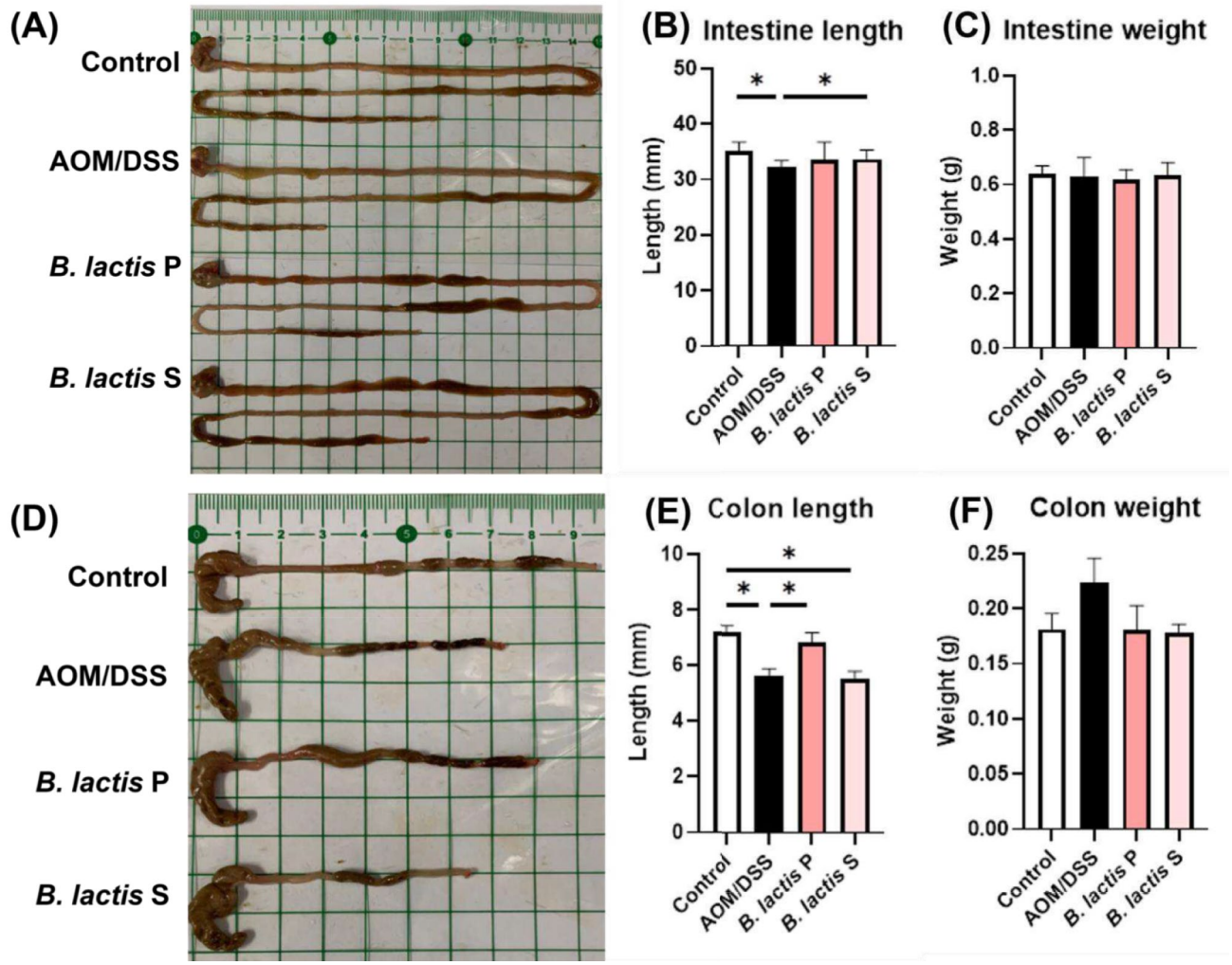

Fig. 3 *B. lactis* P and *B. lactis* S attenuated the AOM/DSS-induced colon shortening. Assessment of the small intestine and the colon length in AOM/DSS murine model on day 79. (**A**) Macroscopic images of the small intestine are shown. (**B**) The small intestine length of each mouse was measured. (**C**) The small intestine weight of each mouse was measured. (**D**) Macroscopic images of the colon are shown. (**E**) The colon length of each mouse was measured. (**F**) The colon weight of each mouse was measured. Data are expressed as the means ± SD. $*p < 0.05$ significantly different from the compared group

Mice treated with AOM/DSS commonly result in colonic precancerous lesions. Histopathological analysis was carried out for the hematoxylin-and-eosin-stained sections of the mice colon. Microscopically, colon samples from the control group show normal histology. In the AOM/DSS group, the colonic sections demonstrate a number of pathological changes: crypts changes in severe lesions throughout mucosa, alteration in the epithelial structure (larger crypts, a thicker and darker-staining epithelial lining, and a larger pericryptal zone), and high levels of inflammatory cell infiltration into the mucosal and submucosal areas. In the *B. lactis* P and *B. lactis* S mice, epithelial lesions and infiltration of inflammatory cells are low as seen in the left panel of Fig. 4E, and the mucosal architecture remains intact when compared to those of the AOM/DSS group, highlighting that *B. lactis* P and *B. lactis* S can prevent or slow down the development of colonic precancerous ACF lesions.

B. lactis modulate hematological, spleen immunological parameters, and inflammatory responses in AOM/DSS-treated mice

In the AOM/DSS group, the total RBC count, hemoglobin, and MCHC are significantly low when compared with those of other groups. In contrast, the total RBC counts, hemoglobin, and MCHC in the mice receiving either the *B. lactis* P or *B. lactis* S treatment remain similar to that of the control

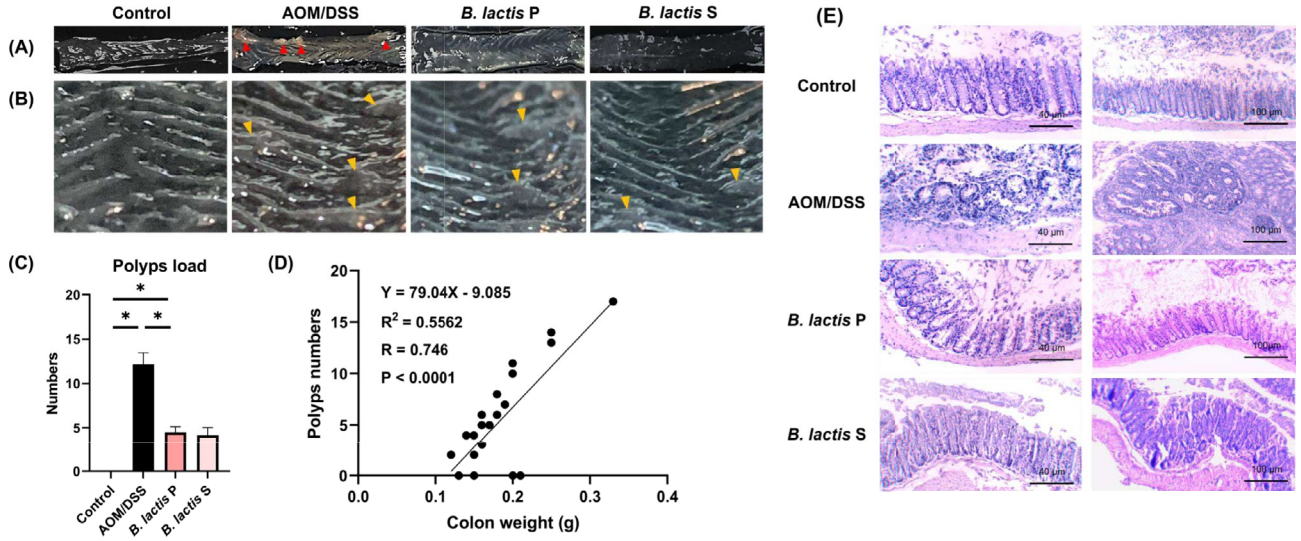

Fig. 4 *B. lactis* P and *B. lactis* S prevented AOM/DSS-induced aberrant crypt foci and the formation of colonic polyps. **A** Representative gross macroscopic image of the colon. Red arrows indicate polyps. **B** Representative pictures of opened specimens by cutting along the bowel. Yellow arrows indicate polyps. **C** The number of polyps per mouse in different parts of small intestines. Data are expressed as the means ± SD. $^{*}p < 0.05$ significantly different from the compared group. **D** Correlation between colon weight and polys number in colons. **E** Representative H&E sections of colons

($p < 0.05$, Fig. 5A), suggesting that *B. lactis* can maintain the level of AOM/DSS-induced RBC, hemoglobin, and MCHC at a steady level.

After the AOM/DSS treatment, the cell counts of absolute neutrophils, eosinophils, and monocytes were determined to be 244.4 ± 144.7, 37.5 ± 19.0, and 181.5 ± 111.0 × 10^9/L, respectively, significantly higher than the counterparts in control. After the administration of *B. lactis* P or *B. lactis* S, the leukocytosis effect was significantly palliated, especially for eosinophilia ($p < 0.05$; Fig. 5B). Figure 6E–H shows the alterations in subpopulation distributions of splenocytes of mice subject to various treatments. The percentage of $CD8^+$ T cells and B cells in splenocytes is meaningfully increased in *B. lactis* P–treated mice (Fig. 5C), suggesting the *B. lactis* treatment promotes acquired immune responses.

To explore the inflammatory modulation of *B. lactis*, we further examined the effects of *B. lactis* P or *B. lactis* S on inflammatory cytokines and NF-κB pathway–related protein expression in the colon tissue of the AOM/DSS-treated mice. The AOM/DSS treatment gave rise to a noticeable elevated level of tumor necrosis factor-α (TNF-α), interleukin (IL)−1β, IL-6, and interferon-γ (IFN-γ) in the colon tissue (Fig. 6A). In contrast, inflammatory cytokines were significantly reduced in the groups with the treatment of *B. lactis* P or *B. lactis* S when compared with those in the AOM/DSS group ($p < 0.05$). In contrast to the AOM/DSS group, where IκBα was decreased and NF-κB was increased, the NF-κB-related inflammation proteins were down-regulated in the *B. lactis* P/*B. lactis* S group, counteracting the effect of AOM/DSS (Fig. 6B, C).

B. lactis mediate the structural and functional compositions of gut microbiota

Since several studies have revealed that there is a close relation between the composition of gut microbiota and inflammation or colonic precancerous lesions (Ryan et al. 2020; Polimeno et al. 2020), we then came to investigate whether gut microbiota of mice were changed upon the *B. lactis* P or *B. lactis* S supplementation during colonic precancerous lesions. The taxonomic profiles at the phylum level revealed that the gut bacteria community in the control mice was dominated by *Bacteroidetes* (64.05 ± 1.86%), *Firmicutes* (31.60 ± 1.12%), and *Deferribacterota* (3.43 ± 1.62%) (Fig. 7A). In the AOM/DSS-treated mice, we found a significant reduction of *Bacteroidetes* (48.93 ± 6.34%) and an increase of *Firmicutes* (42.19 ± 8.16) in the gut microbiota. Clearly, treatment with *B. lactis* P or *B. lactis* S promotes a decrease in *Firmicutes* and *Deferribacterota* while increasing *Bacteroidetes* compared to the AOM/DSS group, ultimately restoring the microbial balance to that of a healthy control group (Fig. 7A). Given that both *Firmicutes* and *Bacteroidetes* are deemed as influential regulators in human gut microbiota (Flemer et al. 2017), the ratio of *Firmicutes* to *Bacteroidetes* (*F*:*B* ratio) acts as an index reflecting intestinal homeostasis. With the AOM/DSS treatment, it significantly increased the population abundance of *Firmicutes*, but the population abundance of *Bacteroidetes* decreased, thus leveraging the *F*:*B* ratio toward *Firmicutes* when compared with that in the control mice ($p < 0.05$; Fig. 7B). Treatment

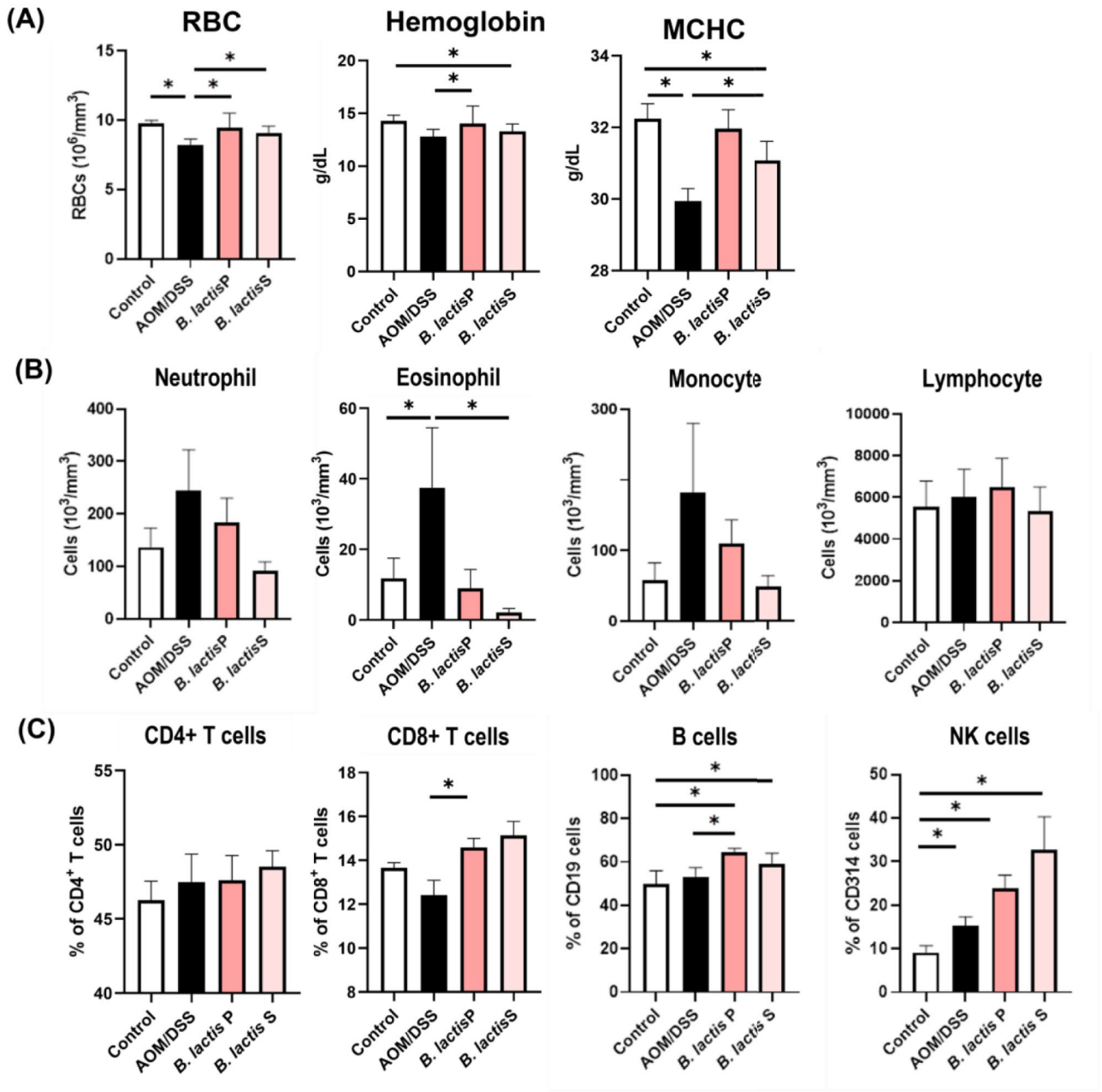

Fig. 5 Effects of *B. lactis* P and *B. lactis* S on the hematological and spleen immunological parameters in AOM/DSS-treated mice. **A** Red blood cell indices. **B** White blood cell indices. **C** Spleenocyte parameter. Data are expressed as the means ± SD. $^*p < 0.05$ significantly different from the compared group

with *B. lactis* P or *B. lactis* S significantly reduced the *F*:*B* ratio compared to the AOM/DSS group, restoring it to the healthy control group level, with *B. lactis* S exhibiting a more pronounced effect. This further suggests that *B. lactis* S supplementation promotes the growth of *Bacteroidetes* in the mouse gut ($p < 0.05$; Fig. 7B). The beta diversity (PCA), the covariance matrix of relative abundance profiles at the genus level, suggested that there is a clear distinction between the control and AOM/DSS groups or the *B. lactis* S and AOM/DSS groups (Fig. 7C). Alpha diversity analysis indicated that the values of the observed species richness estimator Chao1 suggest there are significant differences between the AOM/DSS and *B. lactis* P groups, as well as the AOM/DSS and *B. lactis* S groups (Fig. 7D). However, the values of the Simpson and Shannon diversity indices show no significant differences among four groups (Fig. 7D).

A heat map from hierarchical clustering analysis based on the top 23 different family taxa shows that there are

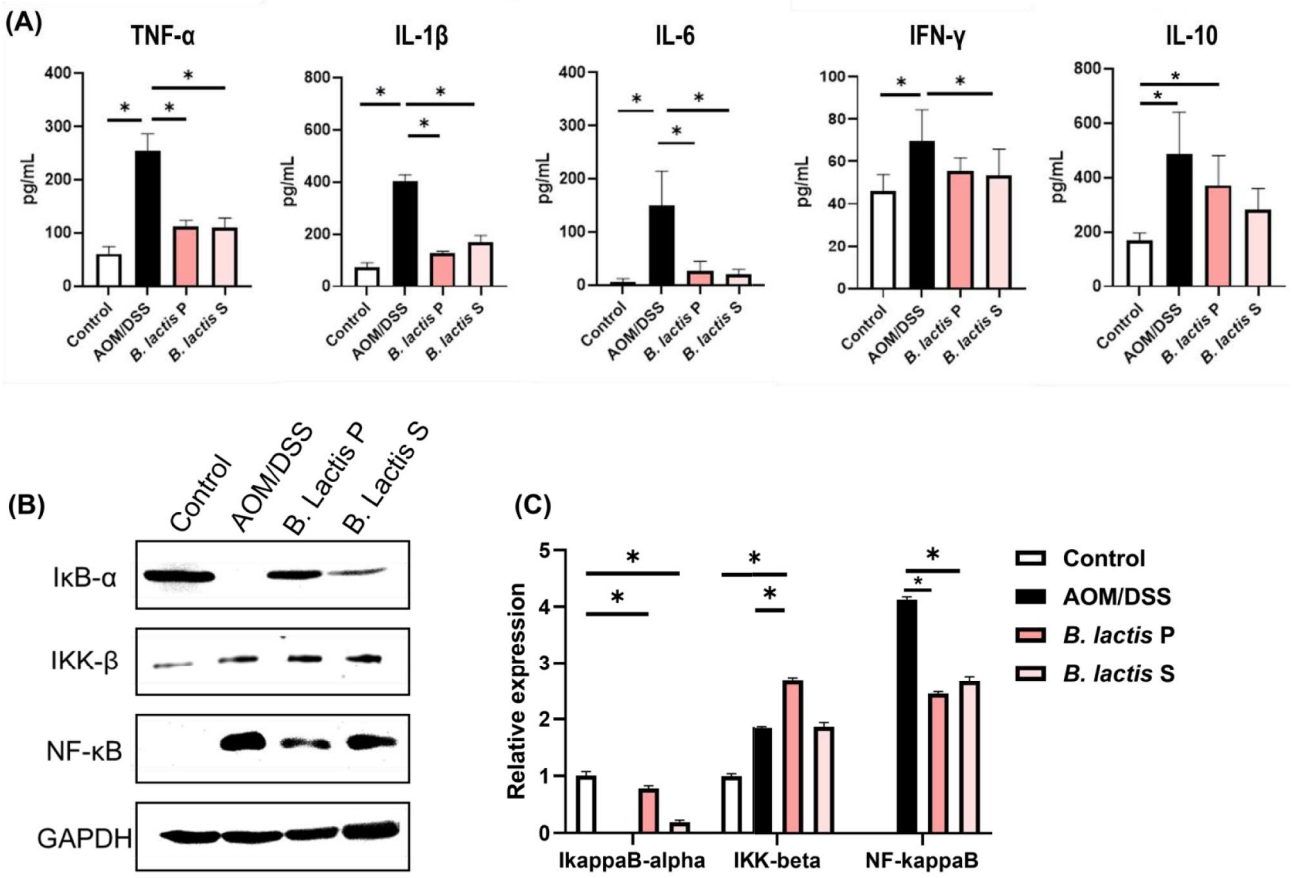

Fig. 6 Effects of *B. lactis* P and *B. lactis* S on expression of inflammatory cytokine and NF-κB signaling in AOM/DSS-treated mice. **A** The protein levels of TNF-α, IL-1β, IL-6, IFN-γ, and IL-10 in the plasma of mice were detected by ELISA. **B** Semiquantitative analysis of colonic tissue protein levels of IκB-α, IKK-β, NF-κB, and GAPDH levels. GAPDH served as an internal control for equal loading. **C** The intensities of western blot bands were determined by the ImageJ. The intensity (mean ± SD) was normalized to the control group that was set to 1. Protein levels differed significantly among the groups, * indicates $p < 0.05$ vs. the compared group

intersample changes amid the four groups. The relatively highly abundant species include *Butyricicoccaceae*, *Oscillospiraceae*, *RF39*, *Clostrida_ vadinBB60*_group, *Acholeplasmataceae*, *Deferribacteraceae*, *Clostridia_UCG-014*, and *Akkermansiaceae* likely as a result of the AOM/DSS treatment, while they were decreased after oral administration of *B. lactis* P or *B. lactis* S (Fig. 7E). In contrast, the relatively less abundant species include *Prevotellaceae*, *Ruminococcaceae*, *Muribaculaceae*, *Rikenellaceae*, and *Tannerellaceae* likewise as a result of the AOM/DSS treatment, which was reversed after oral administration of *B. lactis* P or *B. lactis* S.

At the genus level, we used a heat map, which was derived from hierarchical clustering analysis on the basis of the top 31 different genus taxa, to summarize intersample changes among the four groups. We found that there is a clear separation in the gut microbiota between the AOM/DSS mice and other groups (Fig. 7F). We then selected 7 differently expressed genera and quantified their expression changes. The application of AOM/DSS treatment significantly reduced the relative abundance of well-characterized beneficial bacteria, including *Muribaculaceae*, *Prevotellaceae_UCG-001*, *Anaerostipes*, and *Ruminococcaceae*, in the gut of mice. However, their relative abundance was significantly increased in mice gavaged with *B. lactis* P or *B. lactis* S ($p < 0.05$; Fig. 7G). In contrast, the abundance of pathogenic bacteria, such as *Mucispirillum*, *Clostridia_UCG-014*, and *Clostridia_vadinBB60*, was significantly increased in the AOM/DSS group. However, this trend was reversed when *B. lactis* P or *B. lactis* S was supplemented ($p < 0.05$; Fig. 7G).

Discussions

In this study, we affirmed that the prophylactic administration of *B. lactis* P or *B. lactis* S is capable of alleviating the AOM/DSS-induced weight loss, lowering the expression of inflammatory cytokines, and diminishing ACF and colonic polyps in an AOM/DSS mouse model. These results are in

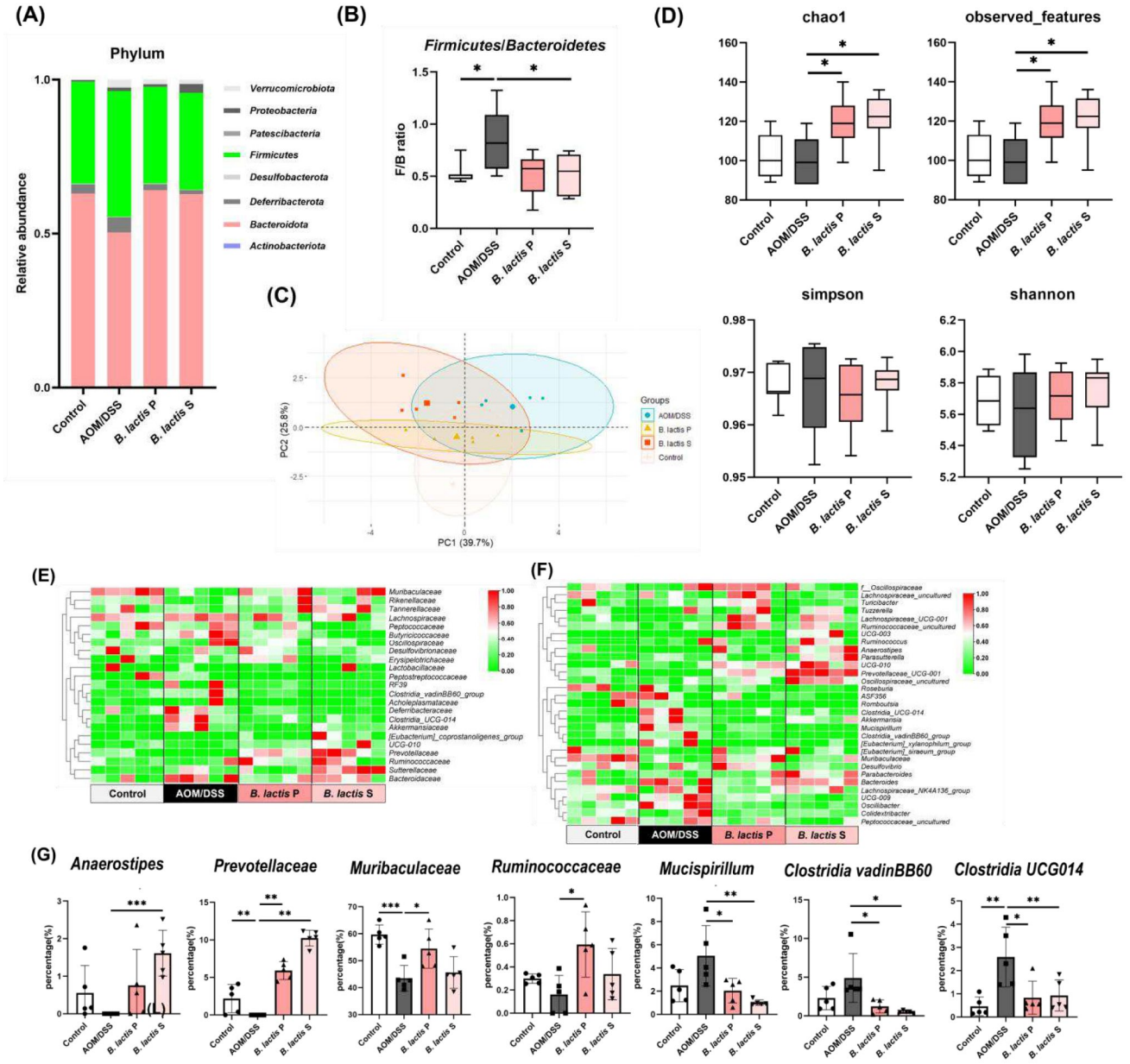

Fig. 7 Effects of *B. lactis* P and *B. lactis* S on the structural and functional composition of gut microbiota. **A** Changes in the relative phylum level abundances of gut microbiota components in AOM/DSS-treated mice. **B** The ratio of *Firmicutes* to *Bacteroidetes* (*F*/*B*) boxplot showing gut microbiota in AOM/DSS-treated mice. Boxes contain 50% of all values and whiskers represent the 25th and 75th percentiles. $*p<0.05$ significantly different from the compared group. **C** PCA plot based on the covariance matrix of genus-level relative abundance of gut microbiota components in AOM/DSS-treated mice. **D** Box plots showing species richness estimator (Chao1 and observed features) and species evenness estimator (Shannon and Simpson) of alpha diversity. $*p<0.05$ significantly different from the compared group. **E**, **F** Heatmap depicting the relative abundance of the most abundant family (**E**) and genera (**F**) (> 0.1%) of gut microbiota from different treatments. The color intensity in each sample is normalized to represent its relative ratio in AOM/DSS-treated mice. A range of colors, from green to red, indicates the relative values of microbiota (0–1). **G** The relative abundance of *Muribaculaceae*, *Prevotellaceae_UCG-001*, *Anaerostipes*, *Ruminococcaceae*, *Mucispirillum*, *Clostridia_UCG-014*, and *Clostridia_vadinBB60*. Data are expressed as the means ± SD. $*p<0.05$, $**p<0.01$, and $***p<0.001$ significantly different from the compared group

good agreement with previous probiotics reports (Genaro et al. 2019; Ni et al. 2017 Rifkin et al. 2020). Interestingly, we identified here that the effect of viable probiotic bacteria and non-viable postbiotic metabolites is comparable, in which the latter achieves a similar inhibitory effect as the former on the AOM/DSS-induced weight loss, inflammation, and precancerous lesions. We reasoned that this outcome is because of the formation of postbiotic metabolites from a

long fermentation process of *B. lactis*, whereby some risk factors are drained out and beneficial factors are converged. Postbiotics are metabolites of microorganisms including short-chain fatty acids (SCFAs), bacterial polysaccharides, and vitamins (B and K), which may act as antioxidant, anti-inflammatory agents, and/or anticancer agents in addition to facilitating the growth of probiotics (Tsilingiri and Rescigno 2013). Although numerous beneficial phenomena for both prebiotics and postbiotics have been learned, new research is still needed as to how and what given metabolites from the cell-free supernatant of *B. lactis* affect the prevention of inflammation and precancerous lesions.

ACF, colon mucosa proliferation, and polyp occurrence are thought to be useful biomarkers/indices for neoplastic lesions in the colon carcinogenetic model (Wargovich et al. 2010). The present study established that high ACF, severe lesions in the mucosa, alterations in epithelial structure, and high-level inflammatory cell infiltration into mucosal and submucosal areas can be induced in the AOM/DSS-treated mice. In contrast, the epithelial lesions, the infiltration of inflammatory cells, and the integrity of mucosal architecture can be significantly improved in the *B. lactis* P and *B. lactis* S mice, suggesting that *B. lactis* P and *B. lactis* S are in a position to compensate the AOM/DSS-induced colonic precancerous lesions. It is known that colonic epithelial inflammation can result in persistent immune dysregulation and neoplastic mucosa; the development of inflammation-associated bowel cancer then follows. A previous study has reported that synbiotic intervention with *L. acidophilus* was able to inhibit colon carcinogenesis by regulating inflammation along with decreasing the number of precancerous lesions on 1,2-dimethylhydrazine (DMH)/DSS-induced colonic precancerous lesions and tumors in mice (Deol et al. 2017; Lee et al. 2019; Li et al. 2019). Moreover, the administration of *Bifidobacterium* was reported able to alleviate intestinal inflammation and carcinogenesis in free fatty acid receptor 2 (Ffar2)-knockout mice (Sivaprakasam et al. 2016), suggesting that bifidobacteria counters oncogenesis through modulating inflammation, restoring compromised mucus layers, and suppressing unfavorable microbiota.

Several lines of evidence have shown that gut microbiota plays an important role in maintaining intestinal homeostasis, as it is closely associated with the development of bowel cancer and bowel precancerous conditions (Polimeno et al. 2020; Ryan et al. 2020). In the present study, we observed that there is a significant population shifting of gut microbiota between the *B. lactis* P/*B. lactis* S mice and AOM/DSS mice, in close correlation to the ratio of *Firmicutes* versus *Bacteroidetes* (Liu et al. 2022). At the phylum level, we found that the *F*:*B* ratio was elevated in the AOM/DSS group, suggesting that AOM/DSS treatment may influence gut microbiota composition during bowel cancer formation by potentially inhibiting the growth of *Bacteroidetes* while favoring the growth of *Firmicutes*. Both *B. lactis* P and *B. lactis* S supplementation, however, can reverse the microbiota imbalance caused by AOM/DSS. At the genus level, the abundance of *Muribaculaceae*, *Prevotellaceae_UCG-001*, *Anaerostipes*, and *Ruminococcaceae* was significantly decreased in the AOM/DSS group. *Muribaculaceae* was shown capable of inhibiting CD8 + T-cell activation to modulate immunity stimulation, therefore being regarded as an anti-inflammatory bacterium (Shang et al. 2021). *Anaerostipes*, *Prevotellaceae*, and *Ruminococcaceae* are considered butyrate-producing bacteria in a way to enhance colonic defense, while the depletion of *Anaerostipes*, *Prevotellaceae*, and *Ruminococcaceae* often leads to the intestinal barrier and gut microbiota dysbiosis (Chen et al. 2022; Dunn et al. 2022; Xie et al. 2022). Lower butyrate production in mucosa and feces of patients is a typical manifestation of bowel cancer, wherefore manipulation of the butyrate level with rebalance of microbiota may point out a new direction in cancer treatment or prevention. The number and abundance of *Muribaculaceae, Prevotellaceae_UCG-001*, *Anaerostipes*, and *Ruminococcaceae* were significantly increased with the *B. lactis* P or *B. lactis* S supplementation, suggesting that *B. lactis* P or *B. lactis* S has a positive role in mediating immune imbalance, colonic inflammation, and development of colonic precancerous lesions. In contrast, *Mucispirillum*, *Clostridia_UCG-014*, and *Clostridia_vadinBB60* were significantly increased in the AOM/DSS group, while the consequence can be corrected with the *B. lactis* P or *B. lactis* S supplementation. *Mucispirillum* is deemed as a mucus-dwelling pathobiont weakening the intestinal barrier integrity as a result of degradation of host-derived mucin. On the other hand, both the genera *Clostridium_UCG-014* and *Clostridia_vadinBB60_group* belong to the *Clostridiaceae* family, which are likely involved in colonic inflammation or cancer (Lin et al. 2022), aging (Saeedi Saravi et al. 2021), and high-fat diet murine models (Zhao et al. 2019) in agreement with our results. Fortunately, the AOM/DSS-induced dysbiosis can be reversed with the *B. lactis* P or *B. lactis* S supplementation.

The schematic representation of the action of *B. lactis* on AOM/DSS-induced colonic precancerous lesions is shown in Fig. 8. The compromised body weight, inflammation, ACF, polyps, and gut dysbiosis were demonstrated in the AOM/DSS-treated mice, for which the *B. lactis* P or *B. lactis* S supplementation significantly reverses the carcinogenesis process and gut dysbiosis, therefore mitigating the weight loss, colon shortening, and inflammatory responses.

In conclusion, the present work sheds new light on the modulatory effect of *B. lactis* P or *B. lactis* S on counteracting inflammation and gut dysbiosis resulting from the AOM/DSS-induced colonic precancerous lesions. Three possible pathways were proposed to account for the *B. lactis* P- or *B. lactis* S–mediated effects against the AOM/

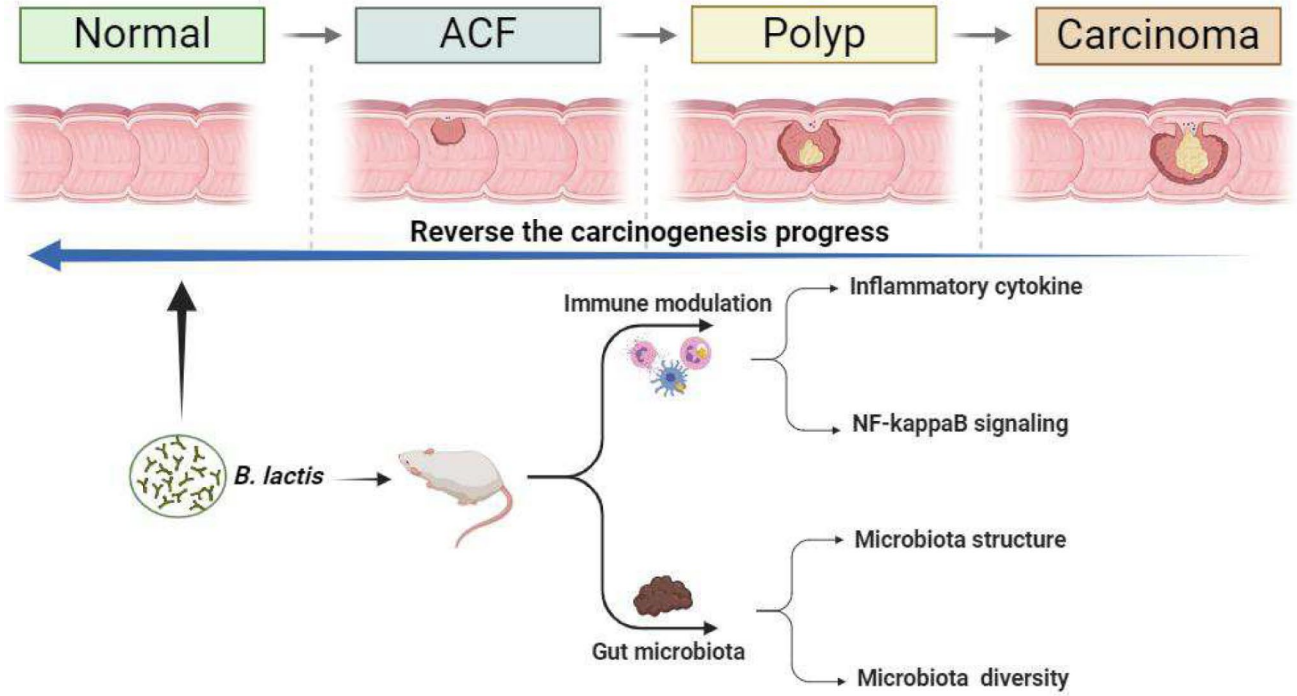

Fig. 8 Schematic of the representative mechanisms for the action of *B. lactis* on AOM/DSS-induced colonic precancerous lesions. In AOM/DSS-treated mice, the body weight, inflammations, ACF, polyps, and gut dysbiosis were enhanced, while the *B. lactis* P or *B. lactis* S administration significantly reversed the carcinogenesis process and gut dysbiosis, as well as mitigated weight losing, colon shorting, and inflammatory response. The present study provided information regarding the *B. lactis* P or *B. lactis* S administration in AOM/DSS-induced colonic precancerous lesions and the regulation of inflammation and gut dysbiosis

DSS-induced colonic precancerous lesions. First, *B. lactis* P or *B. lactis* S is in a position to slow down body weight loss, colon shortening, and formation of ACF and polyps. Second, *B. lactis* P or *B. lactis* S is capable of modulating immune responses via suppression of inflammatory immune cells, pro-inflammatory cytokines, and the NF-κB signaling pathway. Third, *B. lactis* P or *B. lactis* S is adept at rebalancing the gut microbiota reversing the AOM/DSS-induced gut dysbiosis. The overall mechanism exerted by *B. lactis* P or *B. lactis* S for the alleviation of the AOM/DSS-induced colonic precancerous lesions is outlined in Fig. 8. We believe that the beneficial effects of *B. lactis* P and *B. lactis* S demonstrated herein should pave a new avenue for better diagnosis, treatment, prognosis, and prevention of colorectal cancer.

Acknowledgements This work was supported by TCI CO., Ltd.

Authors' contribution CJW and YHC designed the research and supervised the project. YLC and JCL conducted the main experiments and contributed to data analysis. TLL provided technical support. CJW and YHC wrote the manuscript. All authors read and approved the manuscript.

Funding This work was supported by MOST 109–2320-B-031–001 from the Ministry of Science and Technology (MOST), Taiwan.

Data availability Data will be made available on request.

Declarations

Ethics approval All protocols in this study were approved by the Institutional Animal Care and Use Committee (IACUC) at National Taiwan Ocean University (NTOU), Keelung, Taiwan (IACUC permit number: IACUC-110035), in compliance with the Guide for the Care and Use of Laboratory Animals published by the US National Institutes of Health.

Conflict of interest The authors declare no competing interests.

References

Amersi F, Agustin M, Ko CY (2005) Colorectal cancer: epidemiology, risk factors, and health services. Clin Colon Rectal Surg 18(3):133–140. https://doi.org/10.1055/s2005-916274

Arnesen H, Müller MHB, Aleksandersen M, Østby GC, Carlsen H, Paulsen JE, Boysen P (2021) Induction of colorectal carcinogenesis in the C57BL/6J and A/J mouse strains with a reduced DSS dose in the AOM/DSS model. Lab Anim Res 37(1):19. https://doi.org/10.1186/s42826-021-00096-y

Bolger AM, Lohse M, Usadel B (2014) Trimmomatic: a flexible trimmer for Illumina sequence data. Bioinformatics 30(15):2114–2120. https://doi.org/10.1093/bioinformatics/btu170

Brenner BM, Stoler DL, Rodriguez L, Karpenko MJ, Swede H, Petrelli NJ, Anderson GR (2007) Allelic losses at genomic instability-associated loci in villous adenomas and adjacent colorectal cancers. Cancer Genet Cytogenet 174(1):9–15. https://doi.org/10.1016/j.cancergencyto.2006.11.001

Butler LM, Sinha R, Millikan RC, Martin CF, Newman B, Gammon MD, Ammerman AS, Sandler RS (2003) Heterocyclic amines, meat intake, and association with colon cancer in a population-based study. Am J Epidemiol 157(5):434–445. https://doi.org/10.1093/aje/kwf221

Callahan BJ, McMurdie PJ, Rosen MJ, Han AW, Johnson AJA, Holmes SP (2016) DADA2: high-resolution sample inference from Illumina amplicon data. Nat Methods 13(7):581–583. https://doi.org/10.1038/nmeth.3869

Chen Y, Liu Y, Wang Y, Chen X, Wang C, Chen X, Yuan X, Liu L, Yang J, Zhou X (2022) Prevotellaceae produces butyrate to alleviate PD-1/PD-L1 inhibitor-related cardiotoxicity via PPARα-CYP4X1 axis in colonic macrophages. J Exp Clin Cancer Res 41(1):1. https://doi.org/10.1186/s13046-021-02201-4

Cheng J, Laitila A, Ouwehand AC (2021) Bifidobacterium animalis subsp. Lactis HN019 effects on gut health: a review. Front Nutr 8:790561. https://doi.org/10.3389/fnut.2021.790561

D'Aimmo MR, Mattarelli P, Biavati B, Carlsson NG, Andlid T (2012) The potential of bifidobacteria as a source of natural folate. J Appl Microbiol 112(5):975–984. https://doi.org/10.1111/j.1365-2672.2012.05261.x

Deol PK, Khare P, Singh DP, Soman G, Bishnoi M, Kondepudi KK, Kaur IP (2017) Managing colonic inflammation associated gut derangements by systematically optimised and targeted ginger extract-*Lactobacillus acidophilus* loaded pharmacobiotic alginate beads. Int J Biol Macromol 105(Pt 1):81–91. https://doi.org/10.1016/j.ijbiomac.2017.06.117

Dunn KA, MacDonald T, Rodrigues GJ, Forbrigger Z, Bielawski JP, Langille MGI, Van Limbergen J, Kulkarni K (2022) Antibiotic and antifungal use in pediatric leukemia and lymphoma patients are associated with increasing opportunistic pathogens and decreasing bacteria responsible for activities that enhance colonic defense. Front Cell Infect Microbiol 12:924707. https://doi.org/10.3389/fcimb.2022.924707

Flemer B, Lynch DB, Brown JM, Jeffery IB, Ryan FJ, Claesson MJ, O'Riordain M, Shanahan F, O'Toole PW (2017) Tumour-associated and non-tumour-associated microbiota in colorectal cancer. Gut 66(4):633–643. https://doi.org/10.1136/gutjnl-2015-309595

Genaro SC, de Souza L, Reis LS, Reis SK, Rabelo Socca EA, Fávaro WJ (2019) Probiotic supplementation attenuates the aggressiveness of chemically induced colorectal tumor in rats. Life Sci 237:116895. https://doi.org/10.1016/j.lfs.2019.116895

Gomes S, Teixeira-Guedes C, Silva E, Baltazar F, Preto A (2022) Colon microbiota modulation by dairy-derived diet: new strategy for prevention and treatment of colorectal cancer. Food Funct 13(18):9183–9194. https://doi.org/10.1039/d2fo01720b

Kanth P, Grimmett J, Champine M, Burt R, Samadder NJ (2017) Hereditary colorectal polyposis and cancer syndromes: a primer on diagnosis and management. Am J Gastroenterol 112(10):1509–1525. https://doi.org/10.1038/ajg.2017.212

Kowalczyk M, Orłowski M, Klepacki Ł, Zinkiewicz K, Kurpiewski W, Kaczerska D, Pesta W, Zieliński E, Siermontowski P (2020) Rectal aberrant crypt foci (ACF) as a predictor of benign and malignant neoplastic lesions in the large intestine. BMC Cancer 20(1):133. https://doi.org/10.1186/s12885-020-6590-4

Lee CW, Chen HJ, Chien YH, Hsia SM, Chen JH, Shih CK (2019) Synbiotic combination of Djulis (*Chenopodium formosanum*) and *Lactobacillus acidophilus* inhibits colon carcinogenesis in rats. Nutrients 12(1):103. https://doi.org/10.3390/nu12010103

Li SC, Lin HP, Chang JS, Shih CK (2019) *Lactobacillus acidophilus*-fermented germinated brown rice suppresses preneoplastic lesions of the colon in rats. Nutrients 11(11):2718. https://doi.org/10.3390/nu11112718

Lin JS, Chiu YH, Lin NT, Chu CH, Huang KC, Liao KW, Peng KC (2009) Different effects of probiotic species/strains on infections in preschool children: a double-blind, randomized, controlled study. Vaccine 27(7):1073–1079. https://doi.org/10.1016/j.vaccine.2008.11.114

Lin H, Ma X, Yang X, Chen Q, Wen Z, Yang M, Fu J, Yin T, Lu G, Qi J, Han H, Yang Y (2022) Natural shikonin and acetyl-shikonin improve intestinal microbial and protein composition to alleviate colitis-associated colorectal cancer. Int Immunopharmacol 111:109097. https://doi.org/10.1016/j.intimp.2022.109097

Liu J, He H, Xu M, Wang T, Dziugan P, Zhao H, Zhang B (2021) Detoxification of oral exposure to benzo(a)pyrene by Lactobacillus plantarum CICC 23121 in mice. Mol Nutr Food Res 65(12):e2001149. https://doi.org/10.1002/mnfr.202001149

Liu J, Dong W, Zhao J, Wu J, Xia J, Xie S, Song X (2022) Gut microbiota profiling variated during colorectal cancer development in mouse. BMC Genomics 23(Suppl 4):848. https://doi.org/10.1186/s12864-022-09008-3

Martinez FA, Domínguez JM, Converti A, Oliveira RP (2015) Production of bacteriocin-like inhibitory substance by *Bifidobacterium lactis* in skim milk supplemented with additives. J Dairy Res 82(3):350–355. https://doi.org/10.1017/S0022029915000163

Mogna L, Nicola S, Pane M, Lorenzini P, Strozzi G, Mogna G (2012) Selenium and zinc internalized by *Lactobacillus buchneri* Lb26 (DSM 16341) and *Bifidobacterium lactis* Bb1 (DSM 17850): improved bioavailability using a new biological approach. J Clin Gastroenterol 46(Suppl):S41–S45. https://doi.org/10.1097/MCG.0b013e318268861d

Ni Y, Wong VH, Tai WC, Li J, Wong WY, Lee MM, Fong FL, El-Nezami H, Panagiotou G (2017) A metagenomic study of the preventive effect of *Lactobacillus rhamnosus* GG on intestinal polyp formation in $Apc^{Min/+}$ mice. J Appl Microbiol 122(3):770–784. https://doi.org/10.1111/jam.13386

Oberg TS, Ward RE, Steele JL, Broadbent JR (2013) Genetic and physiological responses of Bifidobacterium animalis subsp. lactis to hydrogen peroxide stress. J Bacteriol 195(16):3743–3751. https://doi.org/10.1128/JB.00279-13

Owens JA, Saeedi BJ, Naudin CR, Hunter-Chang S, Barbian ME, Eboka RU, Askew L, Darby TM, Robinson BS, Jones RM (2021) *Lactobacillus rhamnosus* GG orchestrates an antitumor immune response. Cell Mol Gastroenterol Hepatol 12(4):1311–1327. https://doi.org/10.1016/j.jcmgh.2021.06.001

Polimeno L, Barone M, Mosca A, Viggiani MT, Joukar F, Mansour-Ghanaei F, Mavaddati S, Daniele A, Debellis L, Bilancia M, Santacroce L, Di Leo A (2020) Soy metabolism by gut microbiota from patients with precancerous intestinal lesions. Microorganisms 8(4):469. https://doi.org/10.3390/microorganisms8040469

Ponz de Leon M, Benatti P, Borghi F, Pedroni M, Scarselli A, Di Gregorio C, Losi L, Viel A, Genuardi M, Abbati G, Rossi G, Menigatti M, Lamberti I, Ponti G, Roncucci L (2004) Aetiology of colorectal cancer and relevance of monogenic inheritance. Gut 53(1):115–122. https://doi.org/10.1136/gut.53.1.115

Porter RJ, Arends MJ, Churchhouse AMD, Din S (2021) Inflammatory bowel disease-associated colorectal cancer: translational risks from mechanisms to medicines. J Crohns Colitis 15(12):2131–2141. https://doi.org/10.1093/eccojcc/jjab102

Potet F, Soullard J (1971) Polyps of the rectum and colon. Gut 12(6):468–482. https://doi.org/10.1136/gut.12.6.468

Rifkin SB, Giardiello FM, Zhu X, Hylind LM, Ness RM, Drewes JL, Murff HJ, Spence EH, Smalley WE, Gills JJ, Mullin GE (2020) Yogurt consumption and colorectal polyps. Br J Nutr 124(1):80–91. https://doi.org/10.1017/S0007114520000550

Ryan FJ, Ahern AM, Fitzgerald RS, Laserna-Mendieta EJ, Power EM, Clooney AG, O'Donoghue KW, McMurdie PJ, Iwai S, Crits-Christoph A, Sheehan D, Moran C, Flemer B, Zomer AL, Fanning A, O'Callaghan J, Walton J, Temko A, Stack W, Jackson L, Joyce SA, Melgar S, DeSantis TZ, Bell JT, Shanahan F, Claesson MJ (2020) Colonic microbiota is associated with inflammation and host epigenomic alterations in inflammatory bowel disease. Nat Commun 11(1):1512. https://doi.org/10.1038/s41467-020-15342-5

Saeedi Saravi SS, Bonetti NR, Pugin B, Constancias F, Pasterk L, Gobbato S, Akhmedov A, Liberale L, Lüscher TF, Camici GG, Beer JH (2021) Lifelong dietary omega-3 fatty acid suppresses thrombotic potential through gut microbiota alteration in aged mice. Iscience 24(8):102897. https://doi.org/10.1016/j.isci.2021.102897

Shang L, Liu H, Yu H, Chen M, Yang T, Zeng X, Qiao S (2021) Core altered microorganisms in colitis mouse model: a comprehensive time-point and fecal microbiota transplantation analysis. Antibiotics (Basel) 10(6):643. https://doi.org/10.3390/antibiotics10060643

Shussman N, Wexner SD (2014) Colorectal polyps and polyposis syndromes. Gastroenterol Rep (Oxf) 2(1):1–15. https://doi.org/10.1093/gastro/got041

Sivaprakasam S, Gurav A, Paschall AV, Coe GL, Chaudhary K, Cai Y, Kolhe R, Martin P, Browning D, Huang L, Shi H, Sifuentes H, Vijay-Kumar M, Thompson SA, Munn DH, Mellor A, McGaha TL, Shiao P, Cutler CW, Liu K, Ganapathy V, Li H, Singh N (2016) An essential role of Ffar2 (Gpr43) in dietary fibre-mediated promotion of healthy composition of gut microbiota and suppression of intestinal carcinogenesis. Oncogenesis 5(6):e238. https://doi.org/10.1038/oncsis.2016.38

Skrzydło-Radomańska B, Prozorow-Król B, Cichoż-Lach H, Majsiak E, Bierła JB, Kosikowski W, Szczerbiński M, Gantzel J, Cukrowska B (2020) The effectiveness of synbiotic preparation containing *Lactobacillus* and *Bifidobacterium* probiotic strains and short chain fructooligosaccharides in patients with diarrhea predominant irritable bowel syndrome-a randomized double-blind, placebo-controlled study. Nutrients 12(7):1999. https://doi.org/10.3390/nu12071999

Stryker SJ, Wolff BG, Culp CE, Libbe SD, Ilstrup DM, MacCarty RL (1987) Natural history of untreated colonic polyps. Gastroenterology 93(5):1009–1013. https://doi.org/10.1016/0016-5085(87)90563-4

Sugimura N, Li Q, Chu ESH, Lau HCH, Fong W, Liu W, Liang C, Nakatsu G, Su ACY, Coker OO, Wu WKK, Chan FKL, Yu J (2021) *Lactobacillus gallinarum* modulates the gut microbiota and produces anti-cancer metabolites to protect against colorectal tumourigenesis. Gut 71(10):2011–2021. https://doi.org/10.1136/gutjnl-2020-323951

Szajewska H, Hojsak I (2020) Health benefits of *Lactobacillus rhamnosus* GG and *Bifidobacterium animalis* subspecies *lactis* BB-12 in children. Postgrad Med 132(5):441–451. https://doi.org/10.1080/00325481.2020.1731214

Takayama T, Katsuki S, Takahashi Y, Ohi M, Nojiri S, Sakamaki S, Kato J, Kogawa K, Miyake H, Niitsu Y (1998) Aberrant crypt foci of the colon as the precursor of adenoma and cancer. N Engl J Med 339(18):1277–1284. https://doi.org/10.1056/NEJM199810293391803

Tsilingiri K, Rescigno M (2013) Postbiotics: what else? Benef Microbes 4(1):101–107. https://doi.org/10.3920/BM2012.0046

Uccello M, Malaguarnera G, Basile F, D'agata V, Malaguarnera M, Bertino G, Vacante M, Drago F, Biondi A (2012) Potential role of probiotics on colorectal cancer prevention. BMC Surg 12(Suppl 1):S35. https://doi.org/10.1186/1471-2482-12-S1-S35

Wargovich MJ, Brown VR, Morris J (2010) Aberrant crypt foci: the case for inclusion as a biomarker for colon cancer. Cancers (Basel) 2(3):1705–1716. https://doi.org/10.3390/cancers2031705

Wasif N, Etzioni D, Maggard MA, Tomlinson JS, Ko CY (2011) Trends, patterns, and outcomes in the management of malignant colonic polyps in the general population of the United States. Cancer 117(5):931–937. https://doi.org/10.1002/cncr.25657

Xi Y, Xu P (2021) Global colorectal cancer burden in 2020 and projections to 2040. Transl Oncol 14(10):101174. https://doi.org/10.1016/j.tranon.2021.101174

Xie J, Li LF, Dai TY, Qi X, Wang Y, Zheng TZ, Gao XY, Zhang YJ, Ai Y, Ma L, Chang SL, Luo FX, Tian Y, Sheng J (2022) Short-chain fatty acids produced by *Ruminococcaceae* mediate α-linolenic acid promote intestinal stem cells proliferation. Mol Nutr Food Res 66(1):e2100408. https://doi.org/10.1002/mnfr.202100408

Zhao ZH, Xin FZ, Xue Y, Hu Z, Han Y, Ma F, Zhou D, Liu XL, Cui A, Liu Z, Liu Y, Gao J, Pan Q, Li Y, Fan JG (2019) Indole-3-propionic acid inhibits gut dysbiosis and endotoxin leakage to attenuate steatohepatitis in rats. Exp Mol Med 51(9):1–14. https://doi.org/10.1038/s12276-019-0304-5